14.5 K Hydrogen Sorption Cooler: Design and Breadboard Tests

H.J.M. ter Brake[1], J.F. Burger[1], H.J. Holland[1], R.J. Meijer[1], A.V. Mudaliar[1], D. Zalewski[1], M. Linder[2]

[1] University of Twente, 7500 AE Enschede, The Netherlands
[2] ESA-ESTEC, The Netherlands

ABSTRACT

At the University of Twente, a 14.5 K hydrogen-based sorption cooler is under development. It can be used as a stand-alone 14.5 K cooler, or as a precooler, e.g., in combination with a 4 K helium-based sorption cooler. The advantage of sorption coolers is the absence of moving parts and, as a result, their vibration-free operation and, potentially, a very long life. A 4.5 K helium-based sorption-cooler stage was developed and built under a previous ESA-TRP contract, and in 2008, a new ESA-sponsored project was started aimed at the development of a hydrogen cooler stage. A demonstrator cooler has been designed that is able to provide 40 mW of cooling at 14.5 K. It requires an input of 5.6 W of electric power to a sorption compressor that uses a 90 K radiator as a heat sink. The required radiator area is 1.9 m^2. The compressor contains two stages consisting of cells filled with activated carbon. The cells are thermally cycled between the heat-sink level of 90 K and about 210 K, causing hydrogen to be periodically adsorbed and desorbed. As a result, hydrogen is pumped from a low-pressure buffer at 0.1 bar to a medium-pressure buffer at 4 bar, and subsequently to the high-pressure side of the cold stage at 50 bar. The flow direction in this process is controlled by passive valves. In the cold stage the working fluid is precooled by a 50 K radiator (0.1 m^2). In this paper, the design of the hydrogen-based sorption cooler is discussed along with breadboard tests on system components. Tests of the effect of gravity on a cold stage running at 14.5 K are included.

INTRODUCTION

The University of Twente is working in a continuing effort on the development of passively precooled sorption coolers. Such coolers have no moving parts and are, therefore, essentially vibration-free. High-pressure gas is supplied by a sorption compressor that operates with a sorber material such as activated carbon. Activated carbon is a material that by its highly porous structure has a very large internal surface so that it can adsorb large quantities of gas. By heating the sorber the gas is desorbed and a high pressure can be established. By expanding this high-pressure gas in a Joule-Thomson (J-T) cold stage, cooling can be obtained. Sorption coolers are a favorite cooling option for space missions that require long-life and vibration-free cooling to low temperatures. A hydrogen (chemi)sorption cooler is currently successfully applied in ESA's Planck mission.[1] (Physi)sorption coolers are considered for use in the cooler chains of ESA's future Darwin mission[2] and the International X-ray Observatory (IXO).

Cryocoolers 16, edited by S.D. Miller and R.G. Ross, Jr.

In a previous ESA-TRP project, we have developed a sorption cooler concept for the Darwin mission.[3,4] A temperature of 4.5 K is required that is established in two steps, see Fig. 1a. First, a sorption cooler operating with hydrogen gas reaches a temperature of 14.5 K. A second sorption cooler operating with helium gas is precooled by this hydrogen stage, and establishes 5 mW of cooling at 4.5 K. The hydrogen compressor is thermally linked to a 90 K radiator heat sink. The hydrogen gas is precooled by a 50 K radiator that also serves as the heat sink for the helium compressor. The two cooler stages need only a few Watts of input power. Apart from a few passive valves, this cooler concept has no moving parts and is, therefore, virtually vibration-free. The absence of moving parts also simplifies scaling down of the cooler to small sizes, and it contributes to achieving a very long lifetime. In addition, the cooler operates with limited DC currents so that hardly any electromagnetic interference is generated. In the previous ESA-TRP project, the helium stage was realized and successfully tested.[3,4]

A new ESA-sponsored project was started in 2008 aiming at the development of the 14.5 K hydrogen cooler.[5] The preliminary design of this cooler was finished in 2009, the detailed design is currently being finalized, and fabrication of the cooler will start soon. In this paper, the detailed design of this cooler is presented, as well as breadboard tests on individual critical components. First, the requirements are reviewed after which the overall system design is discussed. Then, in three subsequent sections the main system components are considered: the sorption compressors, the check valves, and the cold stage.

COOLER REQUIREMENTS

The most relevant requirements and environmental constraints for the hydrogen-stage cooler are listed in Table 1[5]. When the project started, ESA requested to consider two cases: a small cooling power of 25 mW for precooling of the 4.5 K helium sorption cooler (see Fig. 1a), or a large cooling power of 300 mW for a stand-alone cooler. It was decided to develop the small version, mainly because this cooler can in a later phase nicely be combined with the previously developed helium sorption cooler to yield the combined cooler of Fig. 1a. An extra requirement was that a relatively large mass of 3 kg could be accommodated at 14.5 K. Analysis learned that the mechanical support structure required to accommodate this mass would result in approximately 10 mW extra thermal load on the 14.5 K platform. In order to maintain a net cooling power of at least 25 mW, the required gross cooling power was increased to 40 mW.

SYSTEM DESIGN

A schematic of the system design is given in Fig. 1b. The sorption compressor consists of two stages, with two sorption cells in the first stage and three in the second stage. The cells are thermally cycled between the heat-sink level of 90 K and 210 K for the first compressor stage and 240 K for the second stage. As a result, hydrogen gas is cyclically adsorbed and desorbed, and thus pumped from the low-pressure buffer (P_L at 0.1 bar) to the medium-pressure buffer (P_M at 4 bar) and subsequently to the high-pressure side of the cold stage (at 50 bar). The gas flow direction in the compressor is controlled by passive valves. Both compressor stages are heat sunk on a single radiator temperature level of 90 K. The average input power is 3.0 W for the 1st compressor stage and 2.5 W for 2nd stage respectively. By splitting the radiator in separate temperature levels for both compressor stages, an

Table 1. Requirements and constraints of the hydrogen-stage sorption cooler.[5]

Cooling capacity @ 14.5 K	25 mW (in the project increased to 40 mW)
Temperature stability:	+/- 25 mK for 24 h
	+/- 50 mK for cooler life time
Life time	5 years in orbit, + 1 year ground test, + 2 years storage
Power consumption (including electronics)	< 100 W
Cooler thermal environment	50 K
Radiator compressor heat-sink levels	around 100 K and 50 K
Cooler mass (excluding electronics)	< 5 kg
Mass on 14.5 K interface	3 kg

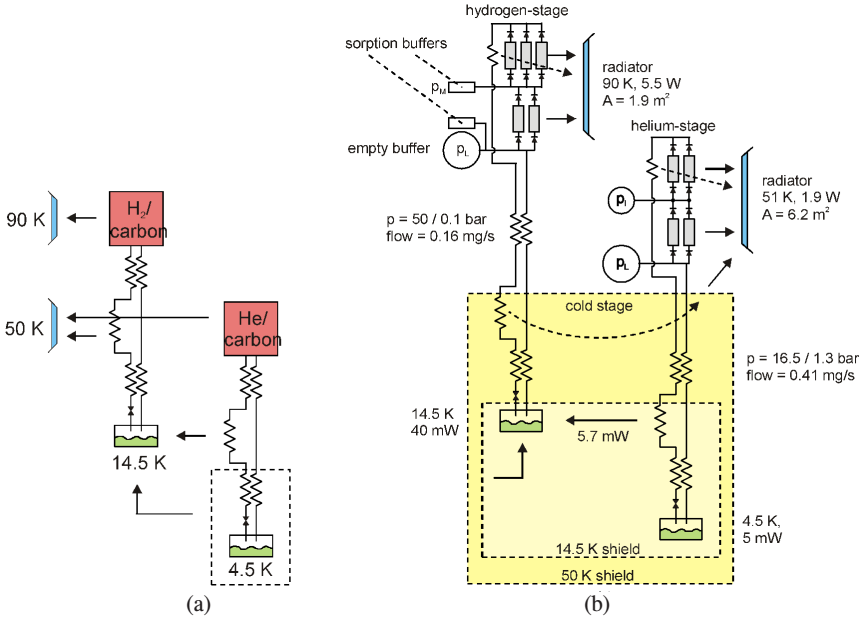

Figure 1. (a) Schematic picture of the proposed helium / hydrogen sorption cooler, which is precooled by two passive radiators at about 50 K and 90 K. (b) Detailed schematic of the helium and hydrogen sorption coolers.

improvement in efficiency (and therefore in size reduction of radiator area) of about 10% can be achieved (optimum temperatures are around 85 K for the first stage and 125 K for the second).

At the system low and medium pressure, buffers are needed to dampen the pressure variation caused by the asynchronous cycling of the sorption cells. A combination is used of relatively small buffers that are filled with activated carbon together with an empty, somewhat larger low-pressure buffer. The 'sorption buffers' are interfaced to the 90 K radiators and have a significant buffer capacity during operation of the sorption cooler to damped the pressure variation. The low-pressure buffer without carbon is used to store the hydrogen gas at high pressure at ambient temperature.

The performance of the cooler was analyzed in detail by a dynamic bondgraph model. In a trade-off study the design parameters were selected in such a way that various parasitic cooler losses (pressure drops, thermal losses, compressor void volume, etc.) are evenly distributed. The total cooler loss due to non-ideal behavior is slightly less than 25%, compared to the ideal cooler performance.

Table 2 gives the estimated mass distribution of the various cooler components.

Table 2. Estimated distribution of the cooler mass.

nr	cooler component	mass (kg)	mass (kg)
1	**total 4 compressor cells + check valves**		**1.3**
	sorption compressor (4 cells of 250 gram each)	1.0	
	check valve units (4 units of 75 g each)	0.3	
2	**cold stage**		**1.0**
3	**total buffer platform (with 3 buffers + 3 pressure sensors)**		**1.61**
	aluminium low-pressure buffer 1 liter	0.5	
	low-pressure buffer with activated carbon, 150 ml	0.3	
	medium-pressure buffer with activated carbon, 25 ml	0.06	
	3 pressure sensors (150 gram each)	0.45	
	aluminium platform + interfacing blocks	0.4	
4	**connecting tubing network + VCR's**		**0.75**
	total cooler, excl. compressor (radiator) platforms & electronics		**4.76**

Notice that the hydrogen stage input power and radiator area can be reduced to 3.5 W and 1.2 m^2, respectively if the original requirement of 25 mW of cooling @ 14.5 K is assumed.

COMPRESSOR CELLS

Fig. 2 shows a cross-sectional diagram of a single cell. The cylindrical stainless steel container of 10 cm in length and 1 cm in diameter with wall thickness of 250 μm is filled with 8.64 g of a very high-density carbon monolith which acts as a sorber. Heating of the carbon is realized with an electric heater placed in the middle of it.

The cavity between the container and the heat sink functions as a gas-gap heat switch. It is 0.1 mm in width and operates with argon. The pressure of argon can be adjusted by active heating and passive cooling of a small carbon pill placed within the gas-gap cavity, allowing for switching of the thermal resistance between the container and the heat sink. When the pressure in the gas-gap is set to 0.1 Pa (off-pressure), the thermal conductivity of argon is negligible and the heat transfer through conduction and radiation from the container to the heat sink dominates (Fig. 3a). This allows for heating the sorber with minimum power losses. Switching the gas-gap to the high thermal conductivity state by increasing the pressure of argon to 400 Pa (on-pressure) creates a strong thermal link between the container and the 90 K heat sink, making the passive cooling of the carbon monolith possible. Maintaining both the low and the high gas-gap pressures at optimized values is critical for the power efficiency of the compressor. High thermal conductivity of the gas gap in the desorption phase of the cycle leads to increased thermal losses in a cell and thus higher power consumption of the compressor (Fig. 3b).

It is expected that the gas-gap cavity will be contaminated during the storage and operation of the compressor by gases other than argon. The primary source of contamination during the storage will be hydrogen permeating through the container walls, with expected partial pressure in the gas gap of 0.5 bar after 2 years of shelf life. Moreover, other mechanisms of contamination will contribute to the overall deterioration of the gas-gap vacuum. To help maintaining the required low-pressure gas-gap conductivity a chemical getter pill (SAES St707) is located in the gas-gap cavity as well. Its purpose is to irreversibly absorb any gaseous contaminations that may be present in the gas gap impairing its function.

Fig. 2b shows the final design of a compressor cell. The cells are identical for both the 1st and the 2nd stages. The material used is 316L stainless steel with the exception of a gas-gap actuator radiation shield and the after-cooler heat sink - both made of copper, the carbon sorbers and the metal hydrate getter pill. The after-cooler, heat-sunk to 90 K, cools down the hot gas leaving a cell to 95 K. The hydrogen getter and the gas-gap actuator are connected to the gas-gap cavity with thin-wall tubes, the lengths of which are optimized to minimize the actuators input powers and switching times.

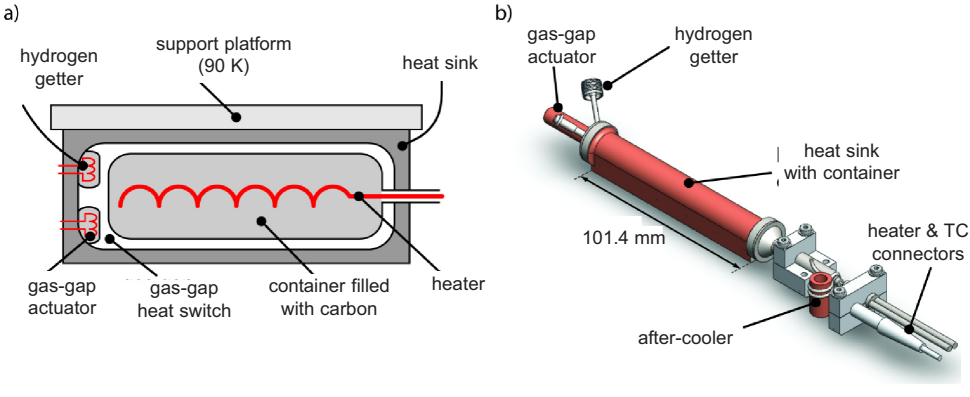

Figure 2. a) Cross-sectional diagram of a single sorption cell with active heating and passive cooling by means of a gas-gap heat switch. b) Design of a sorption compressor cell.

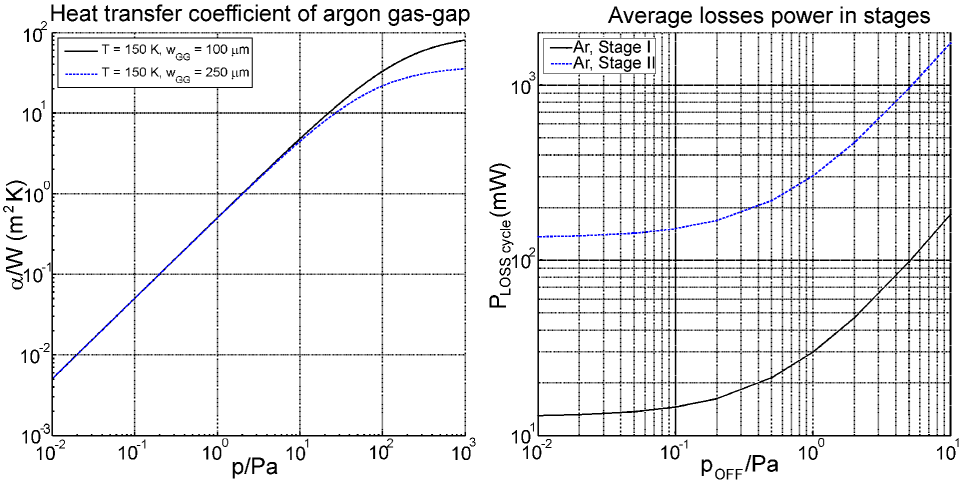

Figure 3. Left (a): Heat transfer coefficient of the argon gas-gap of 100 μm and 250 μm in width. Right (b): thermal losses in compressor stages as a function of the gas-gap argon pressure in the heat-up phase.

CHECK VALVES

The check valve is one of the vital components in the cooling stage of H_2 based sorption compressors. The check valves are used to control the flow direction of hydrogen from the compressor to the cold stage. The losses in the check valves are critical for systems performance, and it directly affects the cooling power. The major losses in the check valves are leak flow and forward flow pressure drop. The input power lost in the compressor due to leak flow can be expressed as

$$P_{loss} = 2\,\beta_1 P_1 + 3\beta_2 P_2 \qquad (1)$$

where P_1 and P_2 are the input powers to the first and second stages, respectively. The factors β give the leak flow rate of a single valve under back pressure, relative to the forward flow rate. The indices 1 and 2 again refer to the two compressor stages. The factors 2 and 3 in the above equation are included because the first stage has two parallel cells and the second stage has three, see Fig. 1b. The input powers to both stages are roughly the same (see in 'System design'). In that case, the relative power lost due to leakage is equal to $b_1 + 1.5\beta_2$. In the system design, a maximum loss of 1% was set as a target. Assuming both valves to have equal flow rates, b should then be below 4.10^{-3}. At a required cooling power of 40 mW, the average forward flow rate is 0.16 mg/s. Therefore, the acceptable leak-flow rate in a single valve is 0.64 μg/s. This rate was set as a target leak-flow limit.

The valves are machined in 316L stainless steel. The valve consists of a seat and a flap for sealing mechanism. The picture of the flap with spring component and the valve seat is show in Fig. 4. The SEM image of the valve seat shows that the central hole is offset, which was due to a manufacturing error and it does not have any impact on leak flow test. The flatness requirements for the valve seat and the flap are very stringent with this flat-on-flat type sealing. Therefore, the flap and the seat have to be extremely clean. Contaminants of the order of 0.5μm would cause the valve to leak above the requirement prescribed. The seat is machined out of a nickel surface deposited on steel. Nickel was preferred for the seat because it can be machined to a high degree of flatness. A layer of gold (around 10 μm) is deposited on the flap and it is then hand polished. The advantage of using a gold layer on the flap is to trap contaminant particles present, if any. A schematic of a typical setup for leak flow test is shown in the Figure 5.

The breadboard testing of valves is carried out at room temperature (300 K) and with helium as working fluid. The acceptable helium leak flow rates at 300 K for the high and low pressure stages, converted from the acceptable hydrogen leak flow rates at 90 K and assuming equal b-values, are

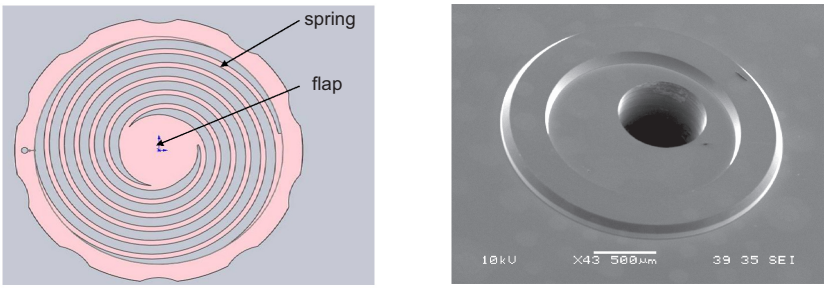

Figure 4. Picture of flap with spring and the valve seat machined on the nickel surface.

0.108 µg/s and 0.175 µg/s, respectively. The breadboard testing of one of the valves is discussed in this section. The valve with seat length of 300µm was tested and the results of the tests are shown in Fig. 6. The filled markers in the plots depict the data points during the pressurizing part of the test and the open markers indicate the bleeding part of the test. It can be seen that during pressurizing the leak flow increases with increase in the pressure difference. There might be a small region where the flap and seat do not seal perfectly due to non-flatness of the seat or the flap, surface roughness, contaminant particles or due to mechanical bending at the center of the flap which causes its edge to lift off from the seat. It can be seen that the valve is leaking well beyond the targeted leak flow limit at the low-pressure stage. On the other hand, leak flow requirements are

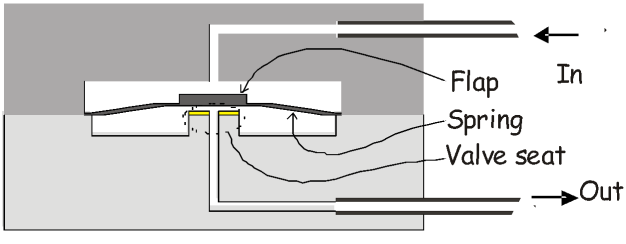

Figure 5. Schematic of leak flow test setup of the check valve

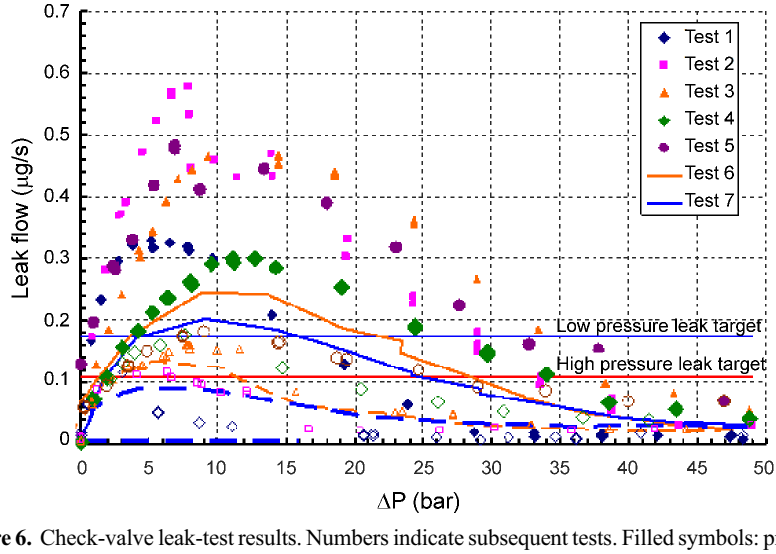

Figure 6. Check-valve leak-test results. Numbers indicate subsequent tests. Filled symbols: pressurizing, open symbols: depressurizing.

achieved for the high pressure stage with this design. It can be seen that during the pressurizing part the leak flow increases first with increase in the pressure difference and then it starts decreasing around a pressure difference of 20 bar. Higher pressure differences mean higher forces acting on the flap and forming a better seal. At higher pressure differences the leak flow drops drastically and is well within the high pressure stage requirements. Once the highest pressure difference is achieved the pressure is bled off slowly. During the bleeding the leak flow starts decreasing initially from 50 bar and then starts increasing at around pressure difference of 25 bars. The force is not sufficient to hold the sealing mechanism between the seat and the flap and then again the leak flow drops down due to the pressure differences. There appeared to be some training effect. The 4^{th} – 7^{th} test perform significantly better than the first. This is not fully understood yet. For the tests 4, 6 and 7, the leak rates at a pressure difference of 4 bar (first compressor stage) and 50 bar (second compressor stage) are around 0.18 µg/s and 0.04 µg/s, respectively. Transferring these data to the 90 K operating point would mean leak rates of 0.66 µg/s at the first stage and 0.24 µg/s at the second. With a forward flow of 0.16 mg/s (40 mW cooling power) we find $\beta_1 = 4.10^{-3}$ and $\beta_2 = 1{,}5.10^{-3}$. Then, the relative power loss due to leakage is $6.5.10^{-3}$, well within the stated requirement of 1%.

The higher leak flow rate at the low-pressure stage is mainly attributed to contamination and the non-flatness of the seat and the flap. Currently research is being carried out to improve in this respect. Also, a small modification in the design of the valve (increasing the seat length) will reduce the leak flow rate in the valve. Increasing the seat length will offer more resistance path to the back flow and increase the surface contact with the flap but at the expense of a slightly larger pressure drop in forward flow direction. New designs are being further explored.

COLD STAGE

The general scheme of the cold stage is depicted in Fig. 7. The counter flow heat exchangers (CFHX) are all configured as tube-in-tube made in stainless steel 316. The heat exchangers (HX) are stainless steel tubing clamped in copper blocks. The aftercooler HX1 is used to cool the gas leaving the compressor to the compressor heat-sink temperature of 90 K. The precooler, HX2, is thermally connected to the 50 K radiator and increases the cooling enthalpy of the cold stage. The aim of the anti-clogging filter (HX3) is to freeze out all remaining impurities just before the gas enters the restriction by cooling the high-pressure gas near to the evaporator temperature. This filter is cooled by a thermal connection to the evaporator (HX4) using a copper strip. Compressed copper foam is used to increase the contact area between fluid and the filter. The temperature in the filter should not decrease below 15.5 K because 50 bar hydrogen solidifies at that temperature. The

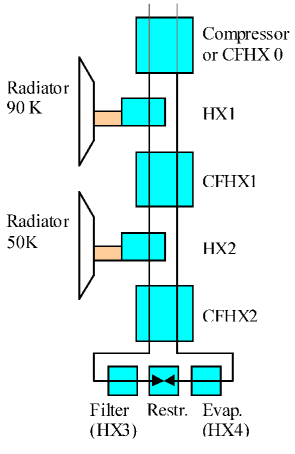

Figure 7. Schematic of the hydrogen cold stage. For test purposes, gas is supplied from a pressurized bottle at 300 K instead of a sorption compressor at 90 K. In this situation, a counter flow heat exchanger is required between 300K and the first radiator at 90 K.

evaporator (HX4) is the main cooling platform. Copper foam is applied to increase the contact area and thus to decrease the temperature difference between the cold liquid hydrogen inside and the copper outside.

A test version of the hydrogen cold stage has been designed, allowing for a somewhat higher flow rate and corresponding cooling power (0.6 mg/s and 150 mW, respectively). High-pressure gas is supplied by a pressurized gas bottle at ambient temperature and, therefore, in the test setup an additional counter flow heat exchanger (CFHX 0) is required. Details on the heat exchangers in this setup were presented elsewhere.[6] The Joule-Thomson flow restriction is a sintered stainless steel plug inside a 1/8" VCR coupling. Compared to the earlier configuration[6] we have removed the thermal link between evaporator and filter. The temperature of the evaporator is measured by a Cernox 1070 high stability temperature sensor (accuracy 6 mK @ 10 K and reproducibility 3 mK). This test version of the cold stage was placed in a vacuum enclosure, in which a 2-stage GM cooler was mounted for cooling HX 1 and HX 2 as well as a thermal radiation shield. High-pressure gas was supplied from a gas bottle and reduced to a pressure of about 50 bar. The outlet of the system was pumped by a 2-stage membrane pump to establish a subatmospheric pressure of around 0.1 bar. This configuration simulates that of the hydrogen sorption cooler as depicted in Fig. 1. In the experiments, HX 1 and HX 2 were stabilized at 90 K and 50 K, respectively. The thermal radiation shield surrounding the whole stage was on average 65 K.

Fig. 8 shows the cold-stage assembly in upward-flow direction. Here, the orientation is vertical such that the restriction is below the evaporator and the liquid has to flow upward. Fig. 9 shows the recorded temperature versus time in this upward-flow configuration. Note that the vertical scale is only 0.2 K. First, no heating power is applied to the evaporator and the lowest temperature is attained. This is the boiling point at the local low pressure in the evaporator, in this case measured to be 14.417 K. The temperature of the evaporator is then controlled to higher values of respectively 14.575, 14.550, 14.525, 14.500 and 14.475 K. The heating power in all cases is about 36 mW. A higher evaporator temperature is established by shifting the liquid-vapor boundary away from the evaporator towards the restriction. However, at the lower temperatures, not all liquid can be evaporated and part of it flows into the return line of CFHX2. Although in this case a very stable evaporator temperature is realized the liquid in the return line cools the high-pressure inflow to such an extent that the hydrogen solidifies and clogs the CFHX flow line (after several hours of operation).

Fig. 10 shows the temperature stability in reversed vertical orientation, in downward flow with the restriction placed above the evaporator. Note that the temperature span is a factor of 10 higher than in Fig. 9. In this case, the boiling point was measured as 14.385 K. The temperature fluctuation at the higher temperatures is larger which is probably due to the fact that liquid produced in the restriction is directly falling on to the evaporator. Therefore, the phase boundary position is much

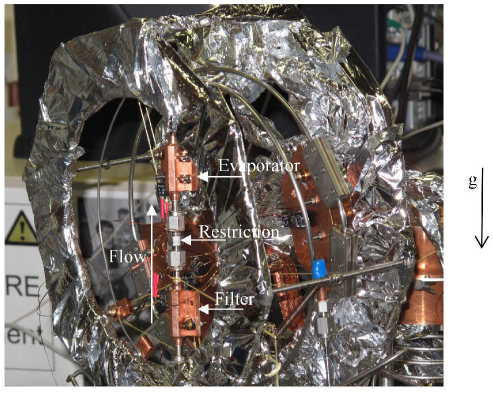

Figure 8. Cold stage assembly in upward flow direction.

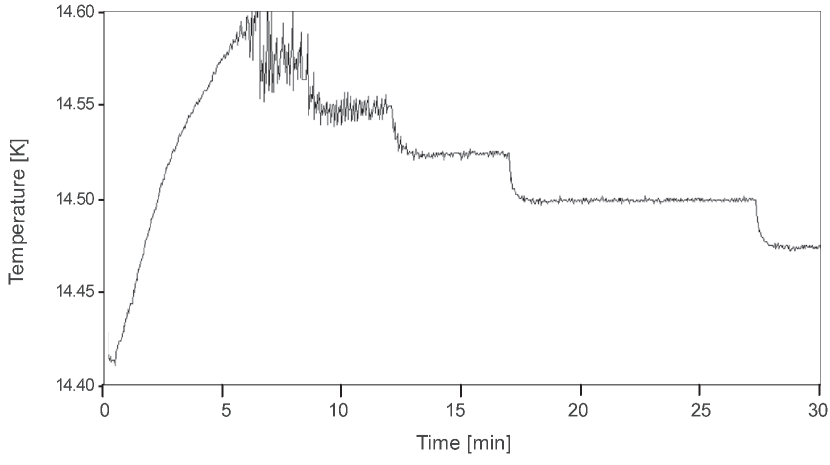

Figure 9. Temperature of the evaporator in upward-flow configuration. The temperature is controlled at various steps in time.

more difficult to control. The required temperature stability is established when the temperature difference between evaporator and boiling liquid is less than about 0.4 K. However, at temperature differences below 0.3 K again clogging of the filter occurs due to freezing of the hydrogen. The controlled heating power in this experiment is about 65 mW.

Based on the above-described breadboard test, we are currently adapting the design of the cold stage. An additional second evaporator will be added to make sure that no liquid enters CFHX2. Furthermore, the restriction will be split into two restriction sections and an additional heater can be placed in between these. A further reason to split the restriction in two parts is that in case of a single restriction (as in the breadboard) the thermal conduction through the restriction material may be so high that the high-pressure end of the restriction is cooled to below 15.5 K and hydrogen freezing may occur.

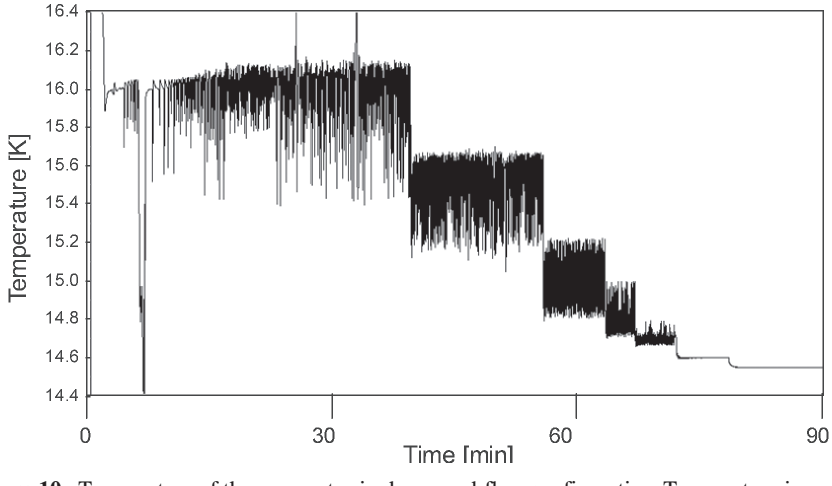

Figure 10. Temperature of the evaporator in downward-flow configuration. Temperature is controlled at various steps in time.

CONCLUSIONS

The design of a 40 mW at 14.5 K hydrogen-based demonstrator sorption cooler was described. The compressor is heat sunk at a 90 K radiator and the hydrogen gas flow is precooled by a 50 K radiator. The compressor consists of two stages, compressing the hydrogen gas from 0.1 bar at the low-pressure end to 4 bar and subsequently to 50 bar. The first stage has two cells in parallel, the second stage has three. All cells are identical and are 10 cm long and 1 cm in diameter. The average mass flow through the system is 0.16 mg/s, requiring an input power of 5.6 W to the compressor. In order to reduce the input power, gas-gap heat switches are used in the compressor cells, operated with argon gas. Passive valves are applied to control the hydrogen flow generated by the compressor cells. An all-metal design is presented based on a flat-to-flat seal. Leak-flow tests at 300 K are presented and showed that the input power loss due to leakage of the valves can be well below 1%.

Breadboard tests were performed on the cold stage and showed stable operation at 14.5 K (within the required 25 mK stability). However, due to freezing of hydrogen at the high-pressure side of the system, the flow is obstructed in long-term operation (several hours). The cold stage design is currently adapted to overcome this problem. Gravity does not affect the stability near the operating point. However, when stabilized at slightly higher temperatures (above about 14.6 K), temperature fluctuations occur due to a varying position of the liquid-vapor phase transition. This effect is obviously influenced by gravity but is not relevant at the cooler operating point of 14.5 K.

REFERENCES

1. Morgante, G., et al., "Cryogenic characterization of the Planck sorption cooler system flight model," *Journal of Instrumentation*, vol. 4 (2009).

2. Burger, J.F., ter Brake, H.J.M., Rogalla, H., Linder, M., "Vibration-free 5 K sorption cooler for ESA's Darwin mission," *Cryogenics*, vol. 42 (2002), pp. 97-108.

3. Burger, J.F., ter Brake, H.J.M., Holland, H.J., Meijer, R.J., Veenstra, T.T., Venhorst, G.C.F., Lozano-Castello, D., Coesel, M., Sirbi, A., "Long-life vibration-free 4.5 K sorption cooler for space applications," *Review of Scientific Instruments*, Vol. 78 (2007).

4. Burger, J.F., Holland, H.J., Meijer, R.J., ter Brake, H.J.M., Doornink, J., Sirbi, A., Linder, M., "Further developments on a vibration-free helium-hydrogen sorption cooler," *Cryocoolers 15*, ICC Press, Boulder, CO (2009).

5 Statement of Work, Hydrogen Sorption Cooler, TEC-MCT/2007/3572/ln/ASP (2007).

6. Burger, J.F., Holland, H.J., Meijer, R.J., Linder, M., ter Brake, H.J.M, "Development of a 15 K hydrogen-based sorption cooler," *Adv. in Cryogenic Engineering*, Vol. 55, Amer. Institute of Physics, Melville, NY (2010), pp. 396-403.